doi:10.1093/brain/awn253 Brain 2009: 132; 124–135 | 124

BRAIN
A JOURNAL OF NEUROLOGY

A deficit of brain dystrophin impairs specific amygdala GABAergic transmission and enhances defensive behaviour in mice

Masayuki Sekiguchi,[1,2] Ko Zushida,[1] Mikiharu Yoshida,[3] Motoko Maekawa,[4] Sari Kamichi,[1] Mizuko Yoshida,[1] Yoshinori Sahara,[5] Shigeki Yuasa,[4] Shin'ichi Takeda[3] and Keiji Wada[1,2]

1 Department of Degenerative Neurological Diseases, National Institute of Neuroscience, National Centre of Neurology and Psychiatry, 4-1-1 Ogawahigashi, Kodaira, Tokyo 187-8502, Japan
2 CREST, Japan Science and Technology Agency, Kawaguchi, Saitama 322-0012, Japan
3 Department of Molecular Therapy, Japan
4 Department of Ultrastructure Research, National Institute of Neuroscience, National Centre of Neurology and Psychiatry, 4-1-1 Ogawahigashi, Kodaira, Tokyo 187-8502, Japan
5 Department of Cell Biology, National Institute of Neuroscience, National Center of Neurology and Psychiatry, 4-1-1 Ogawahigashi, Kodaira, Tokyo 187-8502, Japan

Correspondence to: Masayuki Sekiguchi,
Department of Degenerative Neurological Diseases,
National Centre of Neurology and Psychiatry,
4-1-1 Ogawahigashi, Kodaira,
Tokyo 187-8502, Japan
E-mail: elec1@ncnp.go.jp; sekiguch@ncnp.go.jp

Duchenne muscular dystrophy (DMD) is accompanied by cognitive deficits and psychiatric symptoms. In the brain, dystrophin, the protein responsible for DMD, is localized to a subset of GABAergic synapses, but its role in brain function has not fully been addressed. Here, we report that defensive behaviour, a response to danger or a threat, is enhanced in dystrophin-deficient *mdx* mice. *Mdx* mice consistently showed potent defensive freezing responses to a brief restraint that never induced such responses in wild-type mice. Unconditioned and conditioned defensive responses to electrical footshock were also enhanced in *mdx* mice. No outstanding abnormality was evident in the performances of *mdx* mice in the elevated plus maze test, suggesting that the anxiety state is not altered in *mdx* mice. We found that, in *mdx* mice, dystrophin is expressed in the amygdala, and that, in the basolateral nucleus (BLA), the numbers of $GABA_A$ receptor α2 subunit clusters are reduced. In BLA pyramidal neurons, the frequency of norepinephrine-induced GABAergic inhibitory synaptic currents was reduced markedly in *mdx* mice. Morpholino oligonucleotide-induced expression of truncated dystrophin in the brains of *mdx* mice, but not in the muscle, ameliorated the abnormal freezing response to restraint. These results suggest that a deficit of brain dystrophin induces an alteration of amygdala local inhibitory neuronal circuits and enhancement of fear-motivated defensive behaviours in mice.

Keywords: GABAergic synapse; scaffolding proteins; dystrophin; defensive behaviour; amygdala

Abbreviations: BLA = basolateral nucleus of amygdala; DMD = Duchenne muscular dystrophy; IPSC = inhibitory postsynaptic current; IQ = intelligence quotient; NE = norepinephrine; PD = postnatal day; WT = wild-type

Received April 9, 2008. Revised September 10, 2008. Accepted September 10, 2008. Advance Access publication October 16, 2008

Introduction

Dystrophin is responsible for a severe muscle disease, Duchenne muscular dystrophy (DMD) (Hoffman *et al*., 1987). It is also expressed at relatively high levels in central neurons (Chelly *et al*., 1988; Lidov *et al*., 1990), but the role of dystrophin in brain function is not fully understood. Non-progressive intellectual and/or cognitive impairment is observed in about one-third of DMD patients (Emery, 1987; Bresolin *et al*., 1994; Wicksell *et al*., 2004). The verbal intelligence quotient (IQ) of DMD patients is significantly lower than that of normal controls, but their performance IQ is normal (Billard *et al*., 1992). Psychiatric disorders, such as autism (Komoto *et al*., 1984), and dysthymic and major depressive disorders (Fitzpatrick *et al*., 1986), are also observed in DMD patients, along with autistic symptoms, self-depreciation, marginalization, minor depression, signs of insecurity, hypochondria, high levels of anxiety and poor adaptation to the environment (Roccella *et al*., 2003; verbal and performance IQs were normal in this group of patients). Pathological examination of the CNS in 21 DMD patients revealed no consistent abnormalities (Dubowitz and Crome, 1969).

In the brain, the cerebral cortex, cerebellum and areas CA1–CA3 of the hippocampus are described to be regions in which dystrophin is expressed (Lidov *et al*., 1990, 1993; Lidov, 1996). The dentate gyrus, thalamus, hypothalamus, basal ganglia, most of brainstem and spinal cord are devoid of dystrophin (Lidov, 1996). In neurons, dystrophin selectively localizes to the postsynaptic membrane of GABAergic synapses (Knuesel *et al*., 1999; Brunig *et al*., 2002; Levi *et al*., 2002). Dystrophin binds to cytoskeletal F-actin and β-dystroglycan via its N-terminal region (Ervasti and Campbell, 1991) and its cysteine-rich and C-terminal domains (Suzuki *et al*., 1992), respectively. β-Dystroglycan forms a membrane-integrated postsynaptic adhesion molecular complex with α-dystroglycan in GABAergic synapses (Levi *et al*., 2002). α-Dystroglycan binds to neurexins, which are presynaptic adhesion molecules (Sugita *et al*., 2001). From these molecular features, dystrophin is thought to be an actin-binding postsynaptic scaffold in a subset of GABAergic synapses (Graf *et al*., 2004; Kang and Craig, 2006).

The dystrophin-deficient *mdx* mouse is a model for human DMD (Bulfield *et al*., 1984). A point mutation in exon 23 of the dystrophin gene produces a premature stop codon in *mdx* mice that abrogates expression of full-length 427-kDa dystrophin (Sicinski *et al*., 1989). The lack of dystrophin induces muscle fibre collapse in *mdx* mice similarly to humans; however, abundant regeneration of muscle fibres compensates for the collapsed muscle in *mdx* mice (Tanabe *et al*., 1986). Consequently, *mdx* mice do not display motor disabilities until at least 6 months of age (Pastoret and Sebille, 1995). This allows for behavioural testing of *mdx* mice in the absence of motor defects. Previous studies suggest that *mdx* mice have deficits in passive avoidance learning (Muntoni *et al*., 1991), retention deficits at long delays in spontaneous alteration and bar-pressing tasks (Vaillend *et al*., 1995) and impairments of memory consolidation in both spatial and non-spatial learning tasks (Vaillend *et al*., 2004). However, *mdx* mice show no abnormalities in the Morris water maze, which evaluates hippocampus-dependent spatial learning (Sesay *et al*., 1996). Although these results suggest that *mdx* mice have deficits in particular memory functions, the emotional aspects of *mdx* mice have not been investigated in detail. The only description of the emotional state of these mice is that they showed normal behaviour in a free exploration and light/dark choice situation (Vaillend *et al*., 1995). Abnormalities of GABAergic synapses in *mdx* mice have also been reported; the numbers of $GABA_A$ receptor $\alpha1$ and $\alpha2$ subunit clusters are reduced in the hippocampi and cerebella, compared with control mice (Knuesel *et al*., 1999). This reduction is not accompanied by change in the number of gephyrin clusters (Knuesel *et al*., 1999). Dystrophin is dispensable for GABAergic synapse differentiation (Brunig *et al*., 2002; Levi *et al*., 2002). Because psychiatric symptoms are reported in DMD patients, as mentioned above, and because decreased $GABA_A$ receptor clustering results in enhanced anxiety and a bias for threat cues (Crestani *et al*., 1999), information on the emotional aspects of *mdx* mice is likely to be significant.

In the present study, we performed three behavioural tests in adult *mdx* mice to examine the impact of dystrophin deficiency upon emotional behaviour, and found that defensive freezing behaviour is enhanced in these mice. We also found that, in *mdx* mice, dystrophin is expressed in the amygdala, and that, in the basolateral nucleus, specific GABAergic synaptic transmission is reduced. Furthermore, we found that the enhancement of defensive behaviour was ameliorated by expression of brain dystrophin via morpholino oligonucleotide-induced skipping of exon 23, suggesting that the enhanced defensive responses were attributed to the deficit of dystrophin in the brain.

Materials and Methods

Animals

As the dystrophin gene is located on chromosome X in the mouse (Bulfield *et al*., 1984), male *mdx* mice and their WT littermates were obtained by mating a dystrophin heterozygote female (+/−) with a male WT mouse (C57BL/10J) and were kept at 2–5 mice/cage (genotype at random). The heterozygote female used was obtained by mating three pairs of male WT (C57BL/10J) mice and homozygote female *mdx* (C57BL/10J*mdx*) mice, both of which were obtained from the Central Institute of Experimental Animals (Kanagawa, Japan). Littermate pairs were used in behavioural tests other than experiments using morpholino oligonucleotides. A tail sample was excised for genotyping after behavioural tests. Thus, experimenters were blind to genotype in behavioural tests. Genotyping was performed using previously described PCR methods (Amalfitano and Chamberlain, 1996). The experiments using morpholino oligonucleotides were performed using age-matched mice, the genotypes of which had been already identified and were known to the experimenters. Throughout experiments, including examination of developmental changes in the sensitivity to restraint, each mouse was used for one test only, and repetitive uses in other tests were avoided. Animal care and ethics approval for the animal experiments are described in Supplementary data.

Behavioural test-1 'restraint'

Mice were restrained by the experimenter by placing the neck between the thumb and index finger, and putting the tail between the third and little fingers. After 10 s, the mouse was released to a cage (24 × 17 cm, surrounded by a 12-cm high wall) containing wood chips that had been placed inside the observation box (illuminated with 80 lx). A camera on the ceiling of the box transferred video to a personal computer. Locomotion and freezing were calculated from the image files obtained during the 5 min after restraint using Image OF (O'Hara & Co. Ltd., Tokyo, Japan), modified software based on the public domain NIH Image program (developed at the U.S. National Institutes of Health and available on the Internet at http://rsb.info.nih.gov/nih-image/). Complete immobilization of the mouse, except for respiration, was regarded as a freezing response (Blanchard and Blanchard, 1972).

Behavioural test-2 'electrical footshock'

Electrical footshock was applied to mice in the same apparatus that we previously used for contextual fear conditioning (Zushida *et al*., 2007). After a 3-min habituation to this apparatus (pre-footshock freezing test), an electrical footshock was delivered from the grid (0.8 mA; 2-s duration; scrambled, twice with a 1-min interval), followed by a 3-min post-footshock freezing test. Twenty-four hours later, the mice were introduced to the same apparatus without shock to test contextual learning for 3 min.

Behavioural test-3 'elevated plus maze'

The elevated plus maze test was performed as described previously (Yamada *et al*., 2002), and the detail is described in Supplementary data.

Immunostaining

Halothane-anaesthetized male mice (70- to 100-days old) were perfused transcardially with 0.1 M phosphate-buffered saline (pH 7.4, PBS) for dystrophin staining. The brains were immediately removed and frozen. Coronal brain sections (20 μm thick) were prepared using a microtome (Leica, Wetzlar, Germany). Sections were post-fixed with 4% paraformaldehyde (PFA, 20 min), washed with PBS (5 min) and treated with 0.1% Triton X-100 in PBS (10 min). After incubation with 1% H_2O_2 in PBS (60 min), sections were incubated with PBS solution containing 1% blocking reagent (TSA kit, Molecular Probes, Carlsbad, CA, USA) for 60 min and with the same solution containing 'mouse to mouse blocking reagent' (ScyTek Laboratories, Logan, UT, USA) for an additional 60 min. Sections were then incubated with monoclonal anti-dystrophin antibody (MAB1692; 1:20 dilution, Chemicon, Temecula, CA, USA) in 1% blocking reagent, washed with PBS and incubated with secondary antibody (horseradish peroxidase-conjugated goat anti-mouse IgG, Molecular Probes). Sections were stained using a tyramide signal amplification kit (Molecular Probes) and examined using a confocal laser-scanning microscope (FV-1000, Olympus, Tokyo, Japan).

Immunostaining for $GABA_A$ receptor α2 subunit and gephyrin was performed using the method previously reported by Fritschy *et al*. (1998) with minor modifications, and the detail is described in Supplementary data.

Electrophysiology

Slice patch clamp recordings were performed as reported previously (Zushida *et al*., 2007; Amano *et al*., 2008), and the detail is described in Supplementary data.

Rescue experiments

The methods for microinjection of morpholino oligonucleotides, analysis of the expression of truncated dystrophin by means of Western blotting, and confirmation of exon-skipping by RT–PCR are described in Supplementary data.

Statistical analysis

Statistical differences between two data groups were assessed using the two-tailed Student's *t*-test.

Results

Altered unconditioned and conditioned defensive behaviours in *mdx* mice

We first applied restraint to examine the emotional responses of *mdx* mice. Restraint is widely used as an emotionally aversive stimulus (Miller and McEwen, 2006). After restraint, mice were released to a cage containing wood chips. These tests were performed with the experimenters blind to genotype (see Materials and methods section). Figure 1 shows the locomotion (A) and freezing (B) behaviours of mice over a 5-min period after very brief (10 s) restraint. We found that wild-type (WT) and *mdx* mice (120- to 130-days old) behaved quiet differently in response to restraint. All *mdx* mice displayed very little locomotor activity (Fig. 1A) and a strong freezing response (Fig. 1B, see also Supplementary Video 1). The frozen posture intermittently persisted longer than 30 min in *mdx* mice, after which time the mice commenced normal movement. In almost all cases, freezing was conducted at the edge or corner of the cage; it appeared that *mdx* mice selected a specific location at which to show freezing responses (see Supplementary Video 1). By contrast, all WT mice began moving immediately after restraint (Fig. 1A and B). The *mdx* mice did not freeze when simply transferred without restraint to the measuring field, and the locomotion time course was essentially identical to that in WT mice (Fig. 1C), suggesting that restraint induces freezing in *mdx* mice. In these simple transfer experiments, total locomotion during a 5-min test session was not significantly different between WT and *mdx* mice (Fig. 1D).

Next, we tested the sensitivity of *mdx* mice to electrical footshock. The freezing response immediately after footshock is utilized as an index of fear-motivated unconditioned defensive response (Pentkowski *et al*., 2006). WT and *mdx* mice (100- to 130-days old) did not show freezing responses when they were introduced into a footshock apparatus (Fig. 1E-Pre), but immediately after footshock, they showed freezing responses (Fig. 1E-Post). The amount of time *mdx* mice spent frozen during a 3-min session was significantly longer than the amount of time WT mice spent in this state ($P = 0.027$, $n = 10$ and 9 for WT and *mdx* mice, respectively,

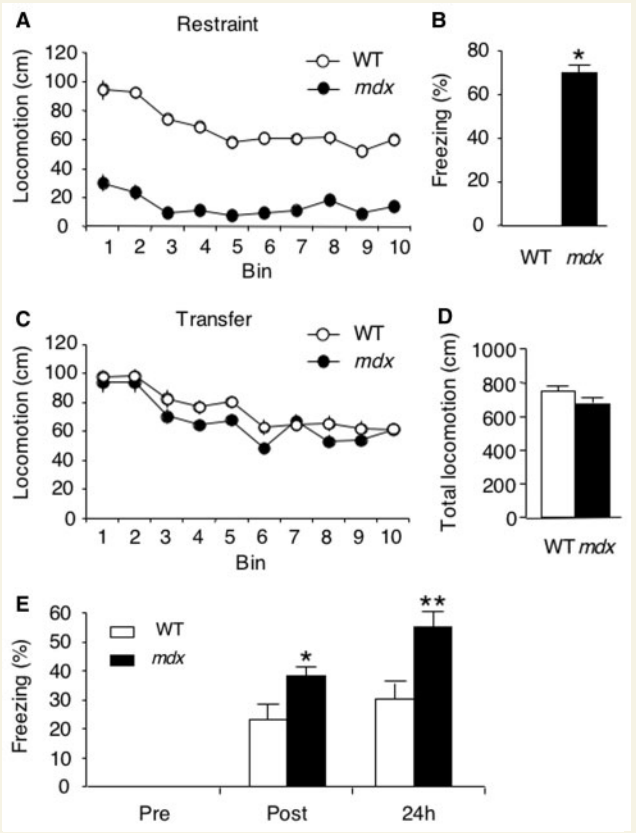

Fig. 1 Adult *mdx* mice exhibit enhanced defensive behaviour. (**A** and **B**) Mice were restrained for a brief (10 s) period and released to a measuring field. Locomotion (**A**, 30-s bins, $n = 18$ for WT and 17 for *mdx* mice for all bins) and freezing time (**B**, $n = 18$ for WT and 17 for *mdx* mice) were measured for 5 min. In **A**, the SEM value was smaller than the symbol where the error bar is not visible. In **B**, the ordinate is the percentage of time mice spent 'frozen'. All values represent means ± SEM $^{*}P < 0.001$ versus WT mice. (**C** and **D**) Mice ($n = 16$ for each group) were transferred without restraint and locomotion was measured for 5 min in 30-s bins. Time-dependent changes in locomotion and total locomotion are presented in (**C**) and (**D**), respectively. (**E**) The percentage of time mice spent 'frozen' during a 3-min test session conducted before, immediately after and 24 h after electrical footshock ($n = 10$ and 9 for WT and *mdx* mice, respectively). $^{*}P = 0.027$, $^{**}P = 0.004$.

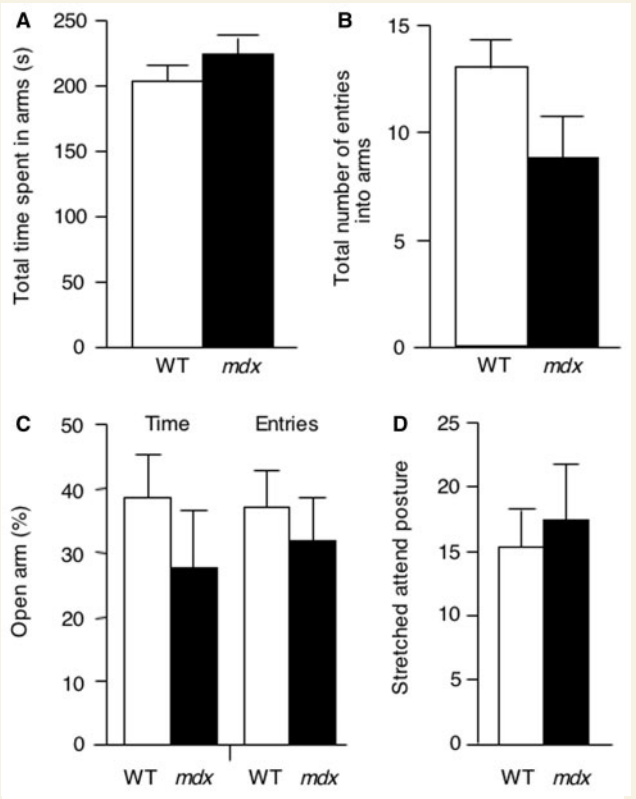

Fig. 2 *Mdx* mice are normal in elevated plus maze tests. Adult WT and *mdx* mice were used. (**A**) Total time mice spent in arms. (**B**) Total number of arm entries. (**C**) Rate of the time mice spent in the open arm and rate of the frequency mice entered into the open arm. (**D**) Number of a stretched attend posture in a central platform. For all, $n = 15$ for WT mice and 11 for *mdx* mice.

two-tailed Student's *t*-test). These conditioned mice were returned to their home cage and, after 24 h, re-exposed to the same apparatus for 3 min to examine their conditioned freezing responses (Fig. 1E-24 h). The freezing rate in this test was also significantly higher among *mdx* mice than among WT mice ($P = 0.004$). These results suggest that fear-motivated unconditioned and conditioned defensive responses were enhanced in *mdx* mice.

Performance in the elevated plus maze is normal

In order to examine anxiety-motivated behaviour in adult *mdx* mice, we used an elevated plus-maze test. The total amount of time the mice spent in the arms, regardless of whether they were open or closed (Fig. 2A), and the total number of entries into arms regardless of their being open or closed (Fig. 2B), were not significantly different between WT and *mdx* mice ($P = 0.303$ and 0.087 for time and entries, respectively), suggesting that *mdx* mice have normal exploratory activity in this test. The percentage of time the mouse spent in the open arm and the percentage of arm visits made to the open arm were not significantly different between WT and *mdx* mice (Fig. 2C, $P = 0.339$ and 0.561 for time and entries, respectively). We also counted the number of times that the mouse adopted a stretched attend posture in the central platform as a risk assessment behaviour (Yamada *et al*., 2002), because risk assessment behaviour is reported to be a defensive behaviour (Blanchard *et al*., 2003). The frequency of stretched attend postures was not significantly different between WT and *mdx* mice (Fig. 2D, $P = 0.642$). These results suggest that WT and *mdx* mice behave identically in the elevated plus maze.

Expression of dystrophin and a reduction in the number of $GABA_A$ receptor clusters in the amygdala

Previous studies have suggested that the organization of an unconditioned freezing response is performed in a brain aversion

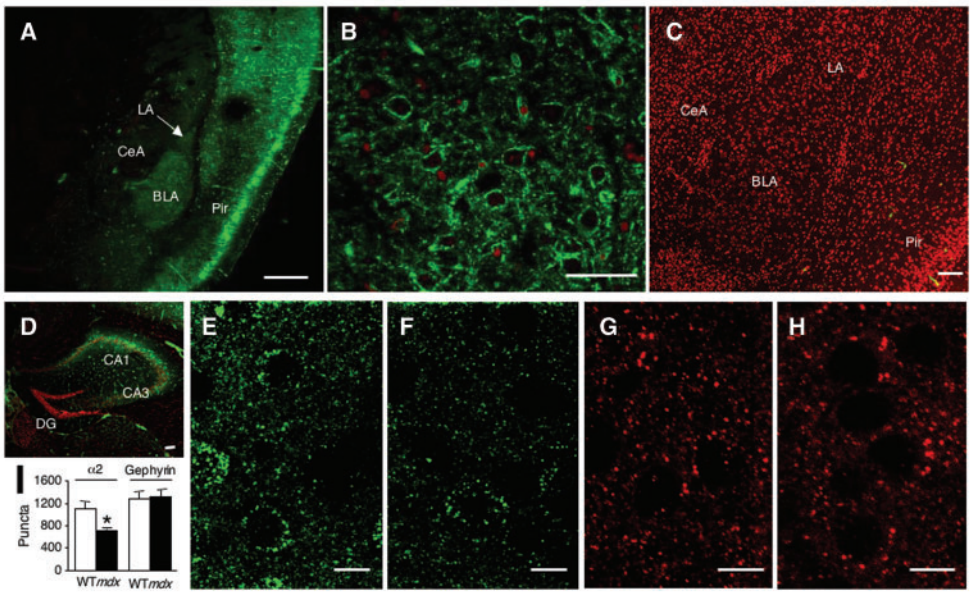

Fig. 3 Dystrophin expression in the amygdala and hippocampus, and a reduction in the number of $GABA_A$ receptor $\alpha2$ subunit clusters in the BLA of *mdx* mice. (**A**–**C**) Dystrophin expression in the amygdala of WT (**A** and **B**) and *mdx* (**C**) mice. Coronal brain sections from adult mice were stained with anti-dystrophin (green) and propidium iodide (red). Scale bars, 500 μm (**A**), 20 μm (**B**) and 100 μm (**C**). (**D**) Dystrophin expression in the hippocampus of a WT mouse. Coronal brain sections from an adult mouse were stained with anti-dystrophin (green) and propidium iodide (red). Scale bars, 100 μm. LA = the lateral nucleus of the amygdala; CeA = the central nucleus of the amygdala; Pir = the piriform cortex; CA1 = the CA 1 field; CA3 = the CA3 field; DG = the dentate gyrus. (**E** and **F**) Staining of the BLA of WT (**E**) and *mdx* (**F**) mice with a $GABA_A$ receptor $\alpha2$ subunit-specific antibody (green). Scale bars, 10 μm. (**G** and **H**) Staining of the BLA of WT (**G**) and *mdx* (**H**) mice with a gephyrin-specific antibody (red). Scale bars, 10 μm. (**I**) The number of the $\alpha2$ subunit and gephyrin clusters in a 6400 μm^2 area in the centre of the BLA. Three images collected with a confocal laser-scanning microscopy (each 1 μm thick) were stacked, and the numbers of green (the $\alpha2$ subunit) and red (gephyrin) dots were counted. Data from five WT and five *mdx* mice for the $\alpha2$ subunit, and from three WT and three *mdx* mice for gephyrin. $^*P = 0.018$ versus WT.

system composed of the medial hypothalamus, the dorsal periaqueductal grey (dPAG) and superior and inferior colliculi (Brandao *et al*., 1999). The hippocampus and amygdala modulate this brain aversion system to alter the extent of the unconditioned freezing response (Pentkowski *et al*., 2006; Ruiz Martinez *et al*., 2006). In addition, projections from the CA1 field and subiculum of the ventral hippocampus to the basolateral nucleus of amygdala (BLA) are involved in contextual fear (Maren and Fanselow, 1995). As mentioned above, dystrophin expression is not detectable in the hypothalamus and most of the brainstem, including the PAG and the superior and inferior colliculi. This information prompted us to assume that the hippocampus and/or amygdala may be affected in *mdx* mice, and that this leads to the emergence of abnormal defensive behaviours. In particular, considering the importance of efferent projections of the amygdala to the PAG in the freezing response induced by fear conditioning (LeDoux *et al*., 1988), the participation of the amygdala was suspected. The expression of dystrophin in the CA1 field of the hippocampus has already been reported, as mentioned above, but there has been no description of dystrophin expression in the amygdala. In order to elucidate whether dystrophin is expressed in the amygdala, we performed immunohistochemical staining of the amygdala using an anti-dystrophin antibody. There was fairly abundant expression of dystrophin (green) in the BLA and the lateral nucleus of the amygdala (LA) in adult WT mice (Fig. 3A). Dystrophin staining in the BLA was punctate along the somatic membrane and processes (Fig. 3B). This pattern is similar to that reported previously for the cerebral cortex (Lidov *et al*., 1990). The BLA and LA of adult *mdx* mice were devoid of immunochemical signals (Fig. 3C), suggesting that the signals in WT mice originated from full-length 427-kDa dystrophin, because *mdx* mice lack only full-length dystrophin, but express its shorter isoforms, Dp140 and Dp71 (Im *et al*., 1996). The distribution of dystrophin-specific immunochemical signals other than in the amygdala was in good agreement with that described in previous reports (Lidov, 1996). In particular, dystrophin expression in the hippocampus was hallmark, being positive in the CA1–CA3 regions and negative in the dentate gyrus (Fig. 3D).

As mentioned in the Introduction section, a previous study showed that the number of $GABA_A$ receptor $\alpha1$ and $\alpha2$ subunit clusters is reduced in the hippocampi and cerebella without being accompanied by change in the number of gephyrin clusters (Knuesel *et al*., 1999). We investigated whether a reduction in the number of $GABA_A$ receptor clusters was evident in the BLA of *mdx* mice. For this purpose, coronal brain slices from adult mice were stained with antibodies specific for the $GABA_A$ receptor $\alpha2$ subunit (green in Fig. 3E and F). Staining with an antibody specific for gephyrin was also performed (red in Fig. 3G and H) for comparison. The $GABA_A$ receptor $\alpha2$ subunit is abundantly expressed in the amygdala (Persohn *et al*., 1992). The $\alpha1$ subunit

is also expressed in the amygdala (Persohn *et al*., 1992), but the cells expressing this subunit are reported to be parvalbumin-containing non-pyramidal neurons (MacDonald and Mascagni, 2004), not pyramidal neurons. Because we found a reduction in GABAergic synaptic transmission in BLA pyramidal neurons (Fig. 4), an analysis of α2 subunit clusters was performed in the present study. As shown in Fig. 3E and F, the immunopositive dots were apparently fewer in the BLA of *mdx* mice compared with WT mice. In contrast, no outstanding differences were evident in the staining of gephyrin (Fig. 3G and H). In the case of the $GABA_A$

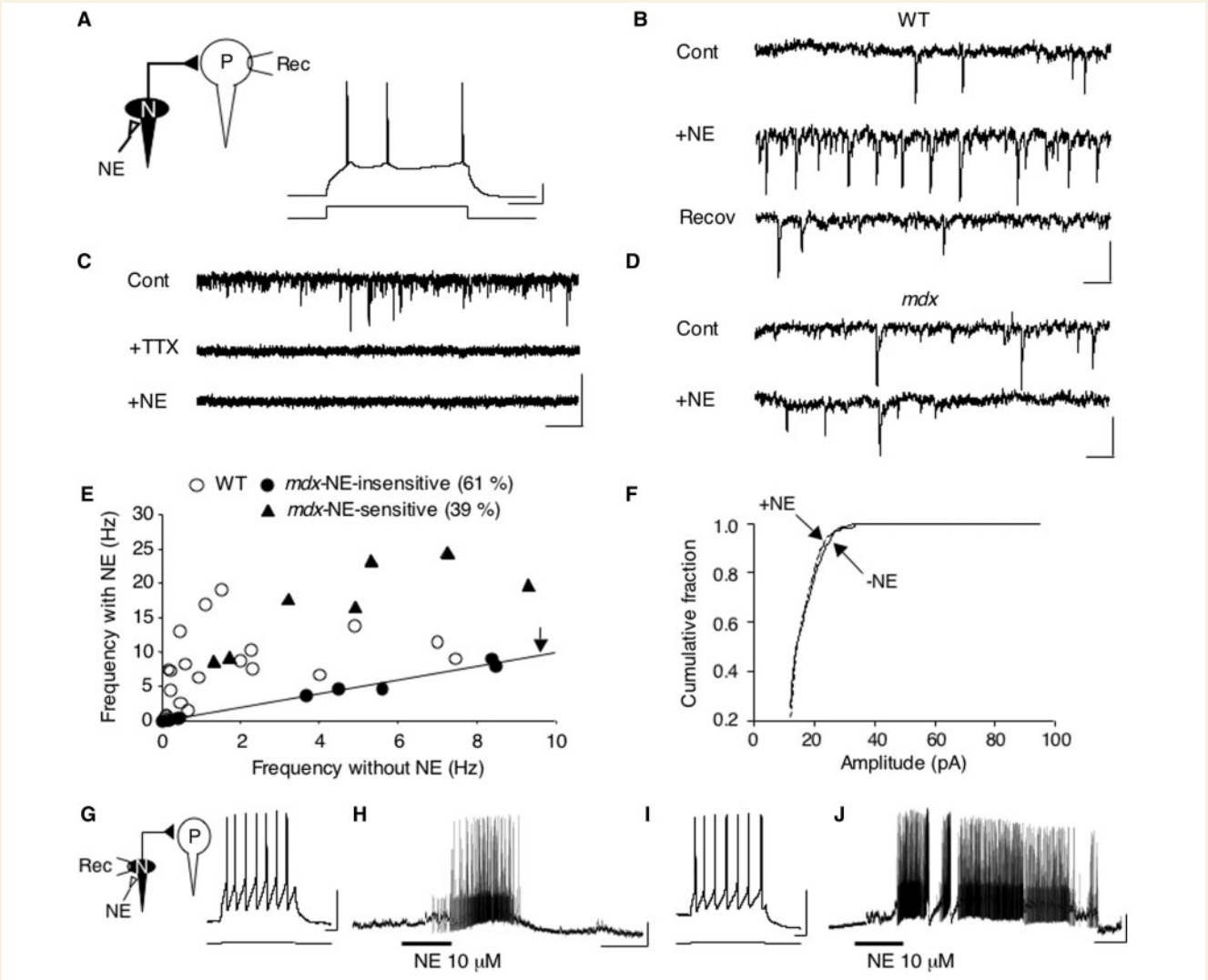

Fig. 4 NE-facilitated GABAergic synaptic transmission is impaired in *mdx* mice. (**A**) A schematic patch clamp recording (Rec) from pyramidal neurons (P) in the BLA. N = non-pyramidal neuron. NE = norepinephrine. The response of an *mdx* mouse pyramidal neuron to a square current pulse (200 pA) delivered via the recording electrode. Resting membrane potential = –65 mV. Scale bar = 200 ms (horizontal) and 20 mV (vertical). (**B**) Sample current traces from a BLA pyramidal neuron of a WT mouse. Control (Cont) and Recovery (Recov) indicate CNQX (20 μM) +MK801 (10 μM); +NE indicates the addition of NE (10 μM). Holding potential = −75 mV. Scale bars = 100 ms and 20 pA. (**C**) Sample traces from a BLA neuron in *mdx* mice demonstrate that induction of IPSCs by NE is greatly suppressed in the presence of TTX (1 μM). Similar results were obtained in WT mice. Scale bars = 1 s and 20 pA. (**D**) Sample recordings from an NE-insensitive BLA pyramidal neuron of *mdx* mice. Holding potential = −75 mV. Scale bars = 100 ms and 20 pA. (**E**) A scatter plot of baseline sIPSC frequency versus the sIPSC frequency in the presence of NE. The line indicated by the arrow indicates equal frequencies with and without NE. (**F**) A cumulative IPSC amplitude histogram in a WT neuron with (+) and without (–) NE. (**G**) Response of a WT non-pyramidal regular spiking neuron to a square current pulse (20 pA) delivered via the recording electrode. Resting membrane potential = –60 mV. Scale bar = 100 ms and 20 mV. Inset, a schematic of patch clamp recording (Rec) from non-pyramidal neurons (N) in the BLA. P = pyramidal neuron. (**H**) Response to bath-applied NE in the same WT neuron. Scale bar = 60 s and 10 mV. (**I**) Response of an *mdx* non-pyramidal regular spiking neuron to a square current pulse (20 pA) delivered via the recording electrode. Resting membrane potential = –59 mV. Scale bar = 100 ms and 20 mV. (**J**) Response to bath-applied NE in the same *mdx* neuron. Scale bar = 60 s and 10 mV.

receptor α2 subunit, the number of immunopositive dots counted in a 6400 μm^2 area in the centre of the BLA was significantly ($P = 0.018$) fewer in *mdx* mice than in WT mice (Fig. 3I, data from five mice of each genotype). In the case of gephyrin, there was no significant difference between *mdx* and WT mice in the number of immunopositive dots similarly counted (Fig. 3I, data from three mice in each mouse model). These results suggest that the number of clusters of the α2 subunit were reduced in the BLA of *mdx* mice without being accompanied by a decrease in the number of clusters of gephyrin.

Electrophysiological abnormalities in BLA pyramidal neurons

In order to examine the effects of dystrophin deficiency on neural activity in the BLA, whole-cell patch clamp recording was performed on pyramidal neurons in acute brain slices. Pyramidal neurons were identified by spike-frequency adaptation in response to depolarizing pulses (Sah *et al*., 2003; Fig. 4A). We elicited action potential-induced GABAergic inhibitory postsynaptic currents (IPSCs) in pyramidal neurons (voltage-clamped at –75 mV) by application of norepinephrine (NE) in the presence of CNQX and MK-801 to block AMPA and NMDA receptors. It has been reported that NE consistently facilitates GABAergic IPSCs in rat BLA pyramidal neurons, mainly via activation of adrenoceptors on the somatodendritic regions of GABAergic interneurons (Braga *et al*., 2004). In our experiments also, application of NE reversibly facilitated the generation of transient inward discharges in all WT BLA neurons tested (Fig. 4B, $n = 17$ from 10 WT mice, mean resting membrane potential = −65.7 ± 0.8 mV, also see Fig. 4E and Table 1). Both the baseline and NE-induced IPSCs were completely blocked by 100 μM picrotoxin, suggesting that these discharges were mediated by $GABA_A$ receptors (data not shown). In the presence of 1 μM tetrodotoxin (TTX), the baseline IPSCs were abolished in all neurons tested (five WT and five *mdx* neurons), and subsequent application of NE did not induce the generation of IPSCs (Fig. 4C). This suggests that the majority of IPSCs were action potential dependent. In contrast to WT neurons, some neurons from *mdx* mice were insensitive to NE (Fig. 4D). Scatter plots of baseline frequency versus the frequency in the presence of NE indicated that there are two types of neurons in *mdx* mice (Fig. 4E). NE-insensitive neurons comprised ~61% (11 out of 18 neurons, data from 11 *mdx* mice, mean resting membrane potential = –65.2 ± 0.7 mV, $n = 18$) of the neurons tested and NE-sensitive neurons comprised 39% of the population (7 out of 18 neurons). Table 1 summarizes the mean (±SEM) frequencies, amplitudes and decay time constants of IPSCs recorded from 17 WT, 11 NE-insensitive *mdx* and 7 NE-sensitive BLA pyramidal neurons. The increase in the frequency of IPSCs induced by NE was significant in WT neurons (1.5 ± 0.5 versus 8.0 ± 1.3) and NE-sensitive *mdx* neurons (5.2 ± 1.0 versus 17.2 ± 2.2), but not in NE-insensitive *mdx* neurons (1.8 ± 0.6 versus 1.7 ± 0.6). NE had no significant effect on the amplitudes or decay time constants of the IPSCs in WT neurons or either type of *mdx* neuron (Table 1). The absence of an effect upon amplitude was also suggested from the cumulative amplitude histogram (Fig. 4F). In the NE-sensitive *mdx* neurons, the baseline (without NE) frequency of IPSCs was about three times higher than that in WT neurons (5.2 ± 1.0 versus 1.5 ± 0.5) and the baseline decay time constant was accelerated compared with WT neurons (6.2 ± 0.6 versus 10.6 ± 0.8). This suggests that NE-sensitive *mdx* neurons are also influenced by the lack of dystrophin, although they are sensitive to NE as well as WT neurons. In term of sensitivity to NE, these results suggest that the induction of IPSCs by NE is reduced in the BLA of *mdx* mice.

Table 1 Frequencies, amplitudes and decay time constants of IPSCs recorded from BLA pyramidal neurons

	n		Frequency (Hz)	Amplitude (PA)	Decay (ms)
WT	17	−NE	1.5 ± 0.5	19.8 ± 1.8	10.6 ± 0.8
		+NE	8.0 ± 1.3$^{\#}$	21.9 ± 2.2	10.9 ± 0.6
Mdx-NE-insensitive	11	−NE	1.8 ± 0.6	20.9 ± 2.8	8.1 ± 1.6
		+NE	1.7 ± 0.6	19.7 ± 2.5	10.9 ± 3.0
Mdx-NE-sensitive	7	−NE	5.2 ± 1.0*	19.5 ± 1.4	6.2 ± 0.6**
		+NE	17.2 ± 2.2$^{\#\#}$	22.0 ± 2.9	7.1 ± 0.9

* $P = 0.008$, ** $P < 0.001$, versus corresponding values in WT mice.
$^{\#}$ $P < 0.001$, $^{\#\#}$ $P = 0.001$, versus corresponding values in −NE.

There are two possible explanations for the reduction of NE-sensitive pyramidal neurons in *mdx* mice. One is a decrease in the number of normal functional GABAergic synapses between NE-responsive interneurons and pyramidal neurons, and another is the impairment of the mechanism by which NE depolarizes interneurons beyond the threshold of action potentials. To clarify this, we recorded from non-pyramidal BLA neurons in brain slices. There are several types of non-pyramidal neuron in the BLA, with respect to their pattern of action potential generation in response to a current pulse (Rainnie *et al*., 2006). We surveyed several cells in WT mice and found that NE induced depolarization with action potentials in so-called regular spiking neurons (Fig. 4G and I). This result is consistent with a report that the major neurons in rat frontal cortex that respond to NE with action potential firing are regular-spiking non-pyramidal neurons (Kawaguchi and Shindou, 1998). Accordingly, we selected these neurons by applying current pulses, and their sensitivity to NE was compared between WT and *mdx* mice. The regular spiking neurons showed a high input resistance (Rainnie *et al*., 2006) in both WT (337.9 ± 58.4 MΩ, $n = 10$) and *mdx* (332.2 ± 46.1 MΩ, $n = 10$) mice. In five out of 10 regular-spiking WT neurons (resting membrane potential = –62.2 ± 1.0 mV, $n = 10$), the NE-induced depolarization was accompanied by action potential firing (Fig. 4H). Similarly, NE induced depolarization with action potentials in five out of 10 *mdx* interneurons tested (Fig. 4J, resting membrane potential = –59.3 ± 0.9 mV, $n = 10$). These results suggest that the proportion of regular-spiking non-pyramidal BLA neurons that respond to NE with action potential firing is identical in WT and *mdx* mice.

Overall, these electrophysiological results suggest that the number of normal functional GABAergic synapses between NE-responsive interneurons and pyramidal neurons is decreased in the BLA of *mdx* mice.

Expression of truncated dystrophin by morpholino oligonucleotide and amelioration of the behavioural phenotype

Our behavioural experiments suggested that defensive behaviour elicited by restraint or footshock is enhanced in *mdx* mice. However, because *mdx* mice lack dystrophin not only in the brain, but also in muscle, there is no direct evidence that these behavioural abnormalities could be attributed to the lack of dystrophin in the brain. In order to elucidate this issue, we took advantage of a morpholino oligonucleotide to induce recovery of dystrophin expression in its truncated form. This morpholino nucleotide induces skipping of exon 23, which includes an aberrant stop codon in the *mdx* allele (Alter *et al*., 2006), producing a 71 amino acid deletion in the mid-rod domain of dystrophin. The rod domain is thought to be a long spacer linking an actin-binding domain near the N-terminus and a dystroglycan-binding domain near the C-terminus of dystrophin, and dystrophin with a deletion within the rod domain is thought to retain the physiological function of full-length dystrophin. Indeed, muscular injection of this morpholino oligonucleotide efficiently ameliorates the muscular pathology of *mdx* mice (Alter *et al*., 2006). In our study, the morpholino oligonucleotide was administered intracerebroventricularly using an osmotic infusion pump that persistently released the drug solution for 1 week. First, we determined the timing of morpholino administration by examining the developmental time course of behavioural abnormalities in *mdx* mice. The restraint-induced freezing response progressed with postnatal development in *mdx* mice (Fig. 5). The freezing response was weak and not significant on postnatal day (PD) 20 ($P = 0.100$ versus WT mice), but was evident on PD36, and gradually increased thereafter. Dystrophin is expressed in the rat cerebral cortex beginning on PD10, and its expression gradually increases thereafter (Kim *et al*., 1992). Therefore, postnatal development of the freezing response coincides with the time course of brain dystrophin expression. The infusion cannula was implanted in *mdx* mice on PD30, the age of onset for the behavioural abnormality.

Intracerebroventricular administration of antisense (indicated as 'A') morpholino oligonucleotide from PD30 induced the appearance of an immunoreactive signal (detected by chemiluminescence) corresponding to dystrophin in Western blots of the postsynaptic density fraction prepared from brain tissue (including the cerebral cortex and amygdala) (Fig. 6A). The immunoreactive signal was evident on PD65 (5-weeks postoperation) and PD80 (7-weeks postoperation), but only trace immunoreactivity was detected on PD55 (3-weeks postoperation) and PD110 (11-weeks postoperation). On PD65 and PD80, the intensity of the band corresponding to dystrophin was estimated to be $27.6 \pm 10.9\%$ ($n = 3$ mice) of the level in WT mice (right most lane in Fig. 6A). In this estimation, samples from WT and *mdx* mice were analysed on the same membrane, and the condition that did not induce saturation of the chemiluminescence signal in WT mice was chosen by stepwisely changing the exposure time for signal detection (see Supplementary Materials and methods).

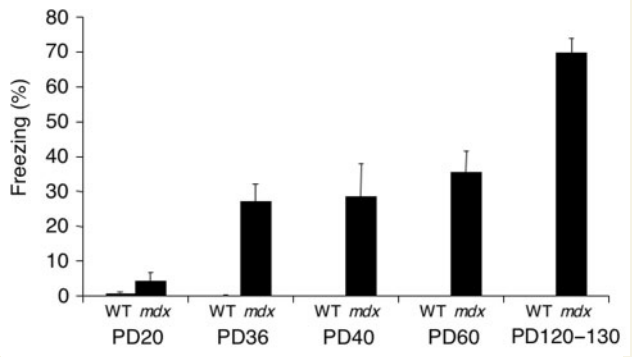

Fig. 5 The enhanced freezing response in *mdx* mice progresses with postnatal development. The amount of time mice spent 'frozen' in response to brief restraint was assessed over a 5-min period on PD20 ($n = 16$ and 15 for WT and *mdx*, respectively), PD36 ($n = 17$ and 12), PD40 ($n = 4$ and 11), PD60 ($n = 8$ and 11) and PD120 to PD130 (reproduced from Fig. 1). With the exception of PD20, values from WT and *mdx* mice differed significantly ($P < 0.0001$).

No signal was detected in samples from mice similarly administered sense (indicated as 'S') morpholino ($n = 5$ mice). Intracerebroventricular administration of sense or antisense morpholino induced no dystrophin expression in the gastrocnemius muscle of *mdx* mice (Fig. 6B). These results suggest that intracerebroventricular administration of antisense morpholino oligonucleotide selectively rescues dystrophin expression in the brain.

Total RNA was isolated from mouse brains administered morpholino (mice were ~65-days old), and nested PCR was carried out using primers that amplify the sequence encoding exons 20–26. Several bands smaller in size than native dystrophin mRNA (indicated as '22-23-24') were evident only in the antisense morpholino-treated *mdx* mouse amygdala, cortex and hippocampus. These bands were not present in the sense morpholino-treated *mdx* mouse cortex, amygdala or in WT mouse cortex (Fig. 6C). As reported for morpholino-treated muscle (Alter *et al*., 2006), the largest band was ~200 bp shorter than the native band, and probably corresponds to a fragment encoding the sequence lacking the 213-bp region encoding exon 23 ('22–24'). The band shorter than the 22–24 band is likely to be a fragment lacking the sequence encoding exons 22 and 23 ('21–24') (Alter *et al*., 2006). These data suggest that the antisense morpholino oligonucleotide induces exon skipping in dystrophin mRNA, thereby recovering expression of truncated forms of dystrophin.

Immunohistochemical analysis of the BLA of WT and morpholino-treated *mdx* mice is shown in Fig. 6D–G. As mentioned above, dystrophin immunoreactivity was abundantly detected in the BLA of WT mice (Fig. 6D). In *mdx* mice treated with antisense morpholino, less dense punctate staining compared with WT mice was observed, as shown in Fig. 6E. Figure 6F shows an image from different slices in the same *mdx* mouse treated with antisense morpholino, focused on two cells in which somatic staining was recovered to the level in WT mice (although such cells were sparse compared with WT mice). Punctate staining was

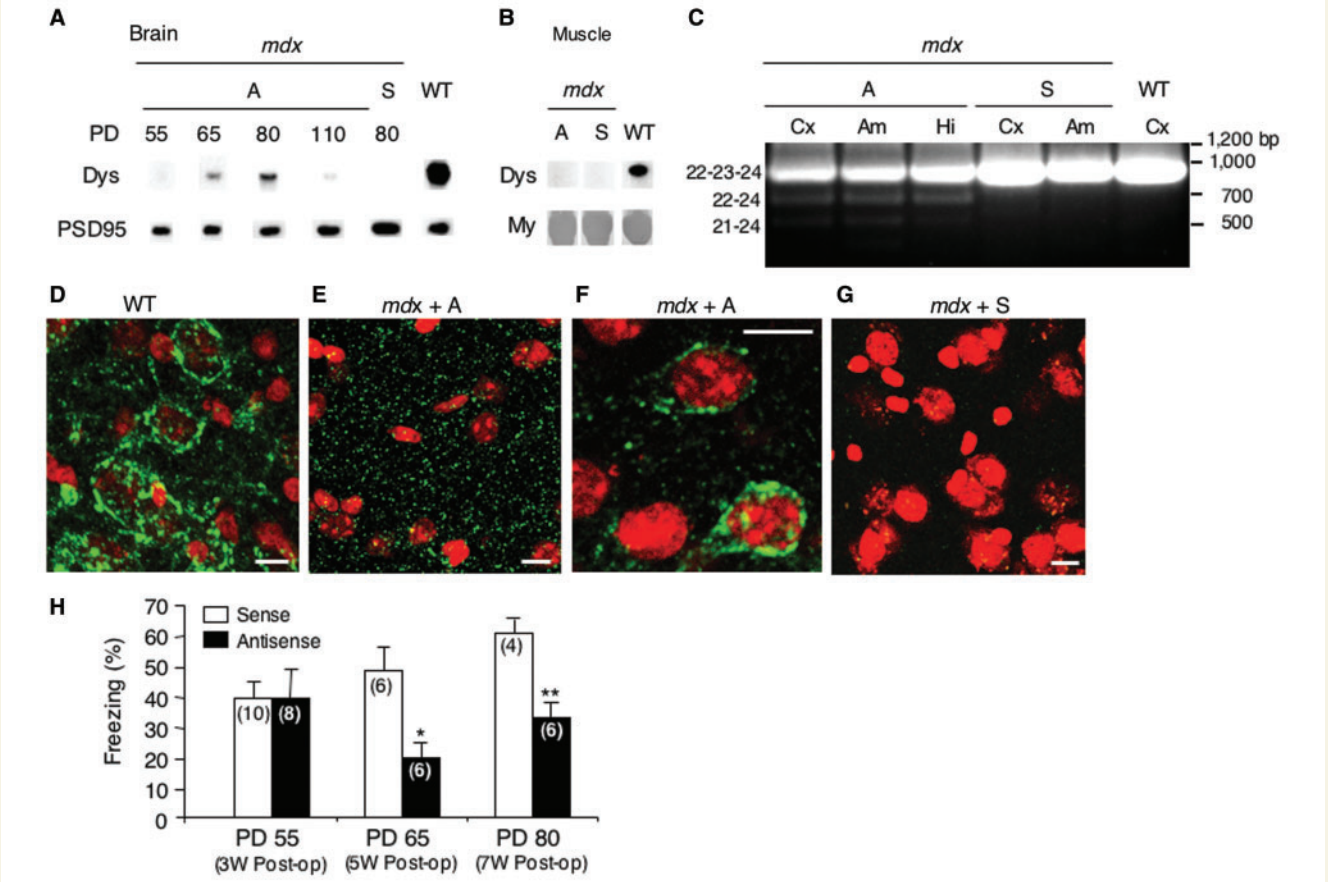

Fig. 6 Morpholino oligonucleotide induces truncated dystrophin expression in the brain. (**A**) Western blot showing the appearance of bands labelled by a dystrophin-antibody of a similar size to native dystrophin in the forebrains of morpholino-treated *mdx* mice (PD55, PD65, PD80 and PD110). From the forebrain, the basal ganglia and hippocampi were removed, and PSD fractions were prepared from the remaining brain tissue. The PSD fractions were Western blotted using anti-dystrophin (Dys) and anti-PSD95 (PSD95) antibodies (as an internal standard). A = antisense morpholino-treated mouse; S = sense morpholino-treated mouse. (**B**) Dystrophin expression in the gastrocnemius muscle isolated from morpholino-treated *mdx* and WT mice (PD80). The 'My' bands represent Coomassie brilliant blue staining for myosin-heavy chain (as an internal standard). (**C**) RT–PCR analysis of total RNA isolated from brain tissue, mainly including cerebral cortex (Cx), amygdala (Am) and hippocampus (Hi) of morpholino-treated *mdx* and WT mice (PD65). A = antisense morpholino; S = sense morpholino. Size markers are shown on the right. The predicted exon configuration for each band is indicated on the left. **(D–G)** Immunohistochemical analysis of dystrophin expression in the BLA of a WT mouse (**D**), an *mdx* mouse treated with antisense morpholino (**E** and **F** are images from different slices in the same *mdx* mouse), and an *mdx* mouse treated with sense morpholino (**G**). Scale bar = 10 μm. (**H**) The restraint-induced freezing response is reduced in antisense morpholino-treated *mdx* mice. The restraint-induced freezing response was measured on PD55 [3 weeks (W) after the brain infusion cannula was implanted], PD65 (5-weeks postoperation) and PD80 (7-weeks postoperation) in sense morpholino- and antisense morpholino-treated mice. Numbers in parentheses indicate the numbers of mice tested. $^{*}P = 0.012$, $^{**}P = 0.005$ versus sense-morpholino-treated mice.

not detected in the BLA of *mdx* mice treated with sense morpholino (Fig. 6G, *mdx* + S).

Next, *mdx* mice were administered morpholino oligonucleotide to examine whether expression of a truncated form of dystrophin reduces the restraint-induced freezing behaviour observed in *mdx* mice. The freezing response was reduced on PD65 and PD80 in conjunction with expression of truncated dystrophin (Fig. 6H, see also Supplementary Videos 2 and 3). The freezing response was not reduced on PD55, when expression of truncated dystrophin was only trace. These results suggest that the behavioural abnormalities in *mdx* mice, at least restraint-induced freezing, can be partially rescued by antisense morpholino oligonucleotide-induced expression of truncated dystrophin in the brain.

Discussion

The results presented here suggest that a deficit of brain dystrophin has an impact on unconditioned and conditioned defensive behaviour in mice. Previous studies suggest that particular memory functions are altered in *mdx* mice. Our present results provide new information that these mice have a severe alteration in particular aspects of emotion in addition to memory functions.

Among emotional defensive behaviours, fear-motivated unconditioned and conditioned defensive responses were altered in *mdx* mice, while anxiety-motivated responses, as assessed by elevated plus maze, were not changed. The amygdala and hippocampus modulate the brain aversion system to alter the extent of the

unconditioned freezing response (Pentkowski *et al*., 2006; Ruiz Martinez *et al*., 2006), and the amygdala is important for association learning, which is necessary for conditioned fear memory (LeDoux, 2000). In terms of abnormal GABAergic synaptic activity in the amygdala, the alteration of fear-motivated unconditioned and conditioned defensive responses in *mdx* mice is consistent with these previous findings, because local GABAergic inhibition is one of the crucial factors regulating amygdala neuronal circuit activity (Sah *et al*., 2003). Indeed, attenuation of GABAergic inhibition in the BLA is known to be correlated with enhancement of conditioned fear memory (Rodriguez Manzanares *et al*., 2005). On the other hand, the absence of an alteration in anxiety behaviour is consistent with a previous report showing that the performance of *mdx* mice in the light/dark box, another test assessing the anxiety state of mice, is similar to those of control mice (Vaillend *et al*., 1995).

Abnormal emotional behaviour has also been reported of mice in which collybistin, another scaffolding protein in GABAergic postsynapses, is deleted (Papadopoulos *et al*., 2007). Collybistin has been implicated in the plasma membrane targeting of gephyrin at glycinergic and GABAergic synapses (Kins *et al*., 2000). These mice show a decrease in miniature IPSC frequency in hippocampal CA1 pyramidal neurons, and impairment of long-term potentiation in CA3-CA1 synapses in the hippocampus, being accompanied by a reduction in the number of gephyrin- and $GABA_A$ receptor γ subunit-immunoreactive puncta in the hippocampus and amygdala. This report and our present results suggest that GABAergic postsynaptic scaffolds are important factors that determine emotional features in mice. In this context, the absence of an alteration in anxiety, as assessed by the elevated plus maze in the *mdx* mice reported here, is in contrast to the severe alterations in performance in the elevated plus maze seen in collybistin-deficient mice (Papadopoulos *et al*., 2007). Differences in the behavioural phenotypes between collybistin-deficient mice and *mdx* mice imply that each GABAergic scaffold protein plays a role in specific emotional behaviour, probably according to its impact upon synaptic activity and the subtype of GABAergic synapses in which it is distributed.

Previous studies suggest that a deficit of dystrophin impairs a subset of GABAergic synapses in the brain. In addition to the above-mentioned marked reduction in the number of $GABA_A$ receptor α1 and α2 subunit clusters in *mdx* mice (Knuesel *et al*., 1999), inhibitory inputs to cerebellar Purkinje cells and long-term depression of the synaptic responses in these cells are reduced in *mdx* mice (Anderson *et al*., 2003*a*, *b*). Destabilization of $GABA_A$ receptors at postsynaptic sites by a deficit of dystrophin is considered to be the mechanism underlying the reduction in the number of receptor clusters (Knuesel *et al*., 1999). Consistently, our results obtained in the BLA also suggested that the number of clusters of α2 subunit and GABAergic synaptic transmission were reduced in *mdx* mice.

A plausible interpretation for the marked reduction in the frequency of NE-induced IPSCs in *mdx* mice is as follows. A reduction in the number of α2 subunit-containing $GABA_A$ receptors would result in attenuation of synaptic responses mediated by this receptor. In the rat BLA, somatostatin-containing non-pyramidal neurons, which respond to NE with action potential firing in rat frontal cortex (Kawaguchi and Shindou, 1998), make synaptic contacts with the distal dendrites of pyramidal cells (Muller *et al*., 2007). In our patch clamp recordings from somata, the synaptic currents generated in distal dendrites are attenuated after being conducted along the long dendrite. Therefore, in the case that the amplitude of current changes in distal dendritic synapses is attenuated because of a reduction in the number of α2 subunit-containing $GABA_A$ receptors in *mdx* mice, the current changes detected in somata cannot be distinguished from baseline noise (about $\pm$5 pA in our experiments), which results in a reduction in the frequency of NE-induced IPSCs recorded from somata. On the other hand, the frequency and amplitude of baseline (without NE) IPSCs were not altered in NE-insensitive *mdx* neurons compared with WT neurons (Table 1). One plausible explanation for this absence of an alteration is that the baseline IPSCs and NE-induced IPSCs are generated in different synapses; for example, baseline IPSCs are generated in synapses between interneurons other than NE-sensitive interneurons and these synapses are not affected by the lack of dystrophin. Consistently, spontaneous bursts of action potentials in interneurons, which generate spontaneous (baseline) IPSCs in pyramidal neurons, are never observed in BLA regular spiking interneurons (Rainnie *et al*., 2006), a subset of which was shown to be NE sensitive in the present study.

Previous reports suggest that NE is released in the amygdala in response to aversive stimuli such as restraint (Tanaka *et al*., 1983) and footshock (Galvez *et al*., 1996). In *mdx* mice, therefore, there is a possibility that the attenuation of BLA NE-induced GABAergic synaptic transmission perturbs the control of excitability of BLA pyramidal neurons in response to aversive stimuli (Braga *et al*., 2004), which inappropriately modulates the brain aversion system in unconditioned defensive behaviour and neuronal circuits for conditioned fear. As mentioned above, somatostatin-containing non-pyramidal neurons make synaptic contacts with the distal dendrites of pyramidal cells (Muller *et al*., 2007); these synapses are often in close proximity to asymmetrical (excitatory) synapses (Muller *et al*., 2007). Because synchronous activation of these excitatory and inhibitory synapses attenuates local depolarization elicited by the excitatory synapses, the spatial relationship of somatostatin-containing inhibitory synapses and excitatory synapses may be an important factor in the perturbation of excitability of BLA pyramidal neurons induced by a deficit of dystrophin.

Although the results of the present study show alterations in BLA GABAergic synapses, impairment in the BLA is not necessarily the only mechanism underlying the alteration of defensive behaviour in *mdx* mice, because dystrophin is also expressed in the CA1 field of the hippocampus. The CA1 field and BLA are connected with each other and their interaction is known to be important for contextual fear memory (Maren and Fanselow, 1995) and hippocampal synaptic plasticity (Nakao *et al*., 2004). Therefore, the impact of a lack of dystrophin in the CA1 region and in an interaction between the CA1 field and the BLA should be investigated for further understanding of the neuronal mechanism underlying abnormal defensive behaviour in *mdx* mice. Regarding the impact on the CA1, Graciotti *et al*. recently suggested that the frequencies of miniature spontaneous IPSCs, not evoked IPSCs, in hippocampal CA1 pyramidal neurons in *mdx* mice

were increased and they propose that the increment is due to presynaptic effects by a dystrophin-deficit (Graciotti *et al*., 2008).

Another piece of information provided in the present study is that a morpholino oligonucleotide that induces expression of truncated dystrophin is able to ameliorate dystrophin deficit-induced alterations in brain function. By comparing DMD patients with spinal muscular atrophy patients, Billard *et al*. (1992) suggested that the mental deficiency in DMD is not secondary to the musculoskeletal handicap. From the point of view that dystrophin deficit in the brain has a direct influence on brain function, the results of our morpholino experiments are in line with this previous report. In the present study, restoration of truncated dystrophin expression to about 30% of the level expressed by WT mice resulted in partial amelioration of the behavioural phenotype in *mdx* mouse brain. It is reported that dystrophin levels as low as 30% of normal are sufficient to avoid muscular dystrophy in humans (Neri *et al*., 2007). Therefore, it is not unreasonable that 30% recovery of dystrophin expression ameliorates the behavioural phenotype. However, as the amelioration of abnormal freezing response was only partial with the expression level we achieved, further improvement in the efficacy of dystrophin expression is necessary for application of morpholino oligonucleotides to therapy for the central nervous system symptoms in human DMD.

Supplementary data

Supplementary data are available at *Brain* online.

Funding

Grants-in-Aid for Scientific Research from the Ministry of Health, Labor and Welfare of Japan (a muscular disease research group, partial); Grants-in-Aid for Scientific Research from the Ministry of Education, Culture, Sports, Science and Technology of Japan; the Program for Promotion of Fundamental Studies in Health Sciences of the National Institute of Biomedical Innovation; Japan Science and Technology Agency.

References

Alter J, Lou F, Rabinowitz A, Yin H-F, Rosenfeld J, Wilton SD, et al. Systemic delivery of morpholino oligonucleotide restores dystrophin expression bodywide and improves dystrophic pathology. Nat Med 2006; 12: 175–77.

Amalfitano A, Chamberlain JS. The *mdx*-amplification-resistant mutation system assay, a simple and rapid polymerase chain reaction-based detection of the *mdx* allele. Muscle Nerve 1996; 19: 1549–53.

Amano T, Wada E, Yamada D, Zushida K, Maeno H, Noda M, et al. Heightened amygdala long-term potentiation in neurotensin receptor type-1 knockout mice. Neuropsychopharmacology [Epub ahead of print March 19, 2008; doi 10.1038/sj.npp.2008.38].

Anderson JL, Head SI, Morley JW. Altered inhibitory input to Purkinje cells of dystrophin-deficient mice. Brain Res 2003a; 982: 280–3.

Anderson JL, Head SI, Morley JW. Long-term depression is reduced in cerebellar Purkinje cells of dystrophin-deficient *mdx* mice. Brain Res 2003b; 1019: 289–92.

Billard C, Gillet P, Signoret JL, Uicaut E, Bertrand P, Fardeau M, et al. Cognitive functions in Duchenne muscular dystrophy: a reappraisal and comparison with spinal muscular atrophy. Neuromuscul Disord 1992; 2: 371–8.

Blanchard RJ, Blanchard DC. Innate and conditioned reactions to threat in rats with amygdaloid lesions. J Comp Physiol Psychol 1972; 81: 281–90.

Blanchard DC, Griebel G, Blanchard RJ. The mouse defense test battery: pharmacological and behavioral assays for anxiety and panic. Eur J Pharmacol 2003; 463: 97–116.

Braga MFM, Aroniadou-Anderjaska V, Manion ST, Hough CJ, Li H. Stress impairs α_{1A} adrenoceptor-mediated noradrenergic facilitation of GABAergic transmission in the basolateral amygdala. Neuropsychopharmacol 2004; 29: 45–58.

Brandao ML, Anseloni VZ, Pandossio JE, De Araujo JE, Castilho VM. Neurochemical mechanisms of the defensive behavior in the dorsal midbrain. Neurosci Biobehav Rev 1999; 23: 863–75.

Bresolin N, Castelli E, Comi GP, Felisari G, Bardoni A, Perani F, et al. Cognitive impairment in Duchenne muscular dystrophy. Neuromuscul Disord 1994; 4: 359–69.

Brunig I, Suter A, Knuesel I, Luscher B, Fritschy JM. GABAergic terminals are required for postsynaptic clustering of dystrophin but not of $GABA_A$ receptors and gephyrin. J Neurosci 2002; 22: 4805–13.

Bulfield G, Siller WG, Wight PAL, Moore KJ. X chromosome-linked muscular dystrophy (*mdx*) in the mouse. Proc Natl Acad Sci USA 1984; 81: 1189–92.

Chelly J, Kaplan J-C, Maire P, Gautron S, Kahn A. Transcription of the dystrophin gene in human muscle and non-muscle tissues. Nature 1988; 333: 858–60.

Crestani F, Lorez M, Baer K, Essrich C, Benke D, Laurent JP, et al. Decreased GABAA-receptor clustering results in enhanced anxiety and a bias for threat cues. Nat Neurosci 1999; 2: 833–9.

Dubowitz V, Crome L. The central nervous system in Duchenne muscular dystrophy. Brain 1969; 92: 805–8.

Emery AEH. Central nervous system. In: Motulsky AG, et al. editors. Duchenne Muscular Dystrophy 2. New York: Oxford University Press; 1987. p. 99.

Ervasti JM, Campbell KP. Membrane organization of the dystrophin-glycoprotein complex. Cell 1991; 66: 1121–31.

Fitzpatrick C, Barry C, Garvey C. Psychiatric disorder among boys with Duchenne muscular dystrophy. Dev Med Child Neurol 1986; 28: 589–95.

Fritschy J-M, Weinmann O, Wenzel A, Benke D. Synapse-specific localization of NMDA and GABAA receptor subunits revealed by antigen-retrieval immunohistochemistry. J Comp Neurol 1998; 399: 194–210.

Galvez R, Mesches MN, McGaugh JL. Norepinephrine release in the amygdala in response to footshock stimulation. Neurobiol Learn Mem 1996; 66: 253–7.

Graciotti L, Minelli A, Minciacchi D, Procopio A, Fulgenzi G. GABAergic miniature spontaneous activity is increased in the CA1 hippocampal region of dystrophic *mdx* mice. Neuromuscul Disord 2008; 18: 220–6.

Graf ER, Zhang X-Z, Jin S-X, Linhoff MW, Craig AM. Neurexins induce differentiation of GABA and glutamate postsynaptic specializations via neuroligins. Cell 2004; 119: 1013–26.

Hoffman EP, Brown RHJ, Kunkel LM. Dystrophin: the protein product of Duchenne muscular dystrophy locus. Cell 1987; 51: 919–28.

Im WB, Phelps SF, Copen EH, Adams EG, Slightom JL, Chamberlain JS. Differential expression of dystrophin isoforms in strains of *mdx* mice with different mutations. Human Molec Genet 1996; 5: 1149–53.

Kang Y, Craig AM. Composition and assembly of GABAergic postsynaptic specializations. In: Dityatev A, El-Husseini A, editors. Molecular mechanisms of synaptogenesis. New York: Springer Science+Business Media LLC; 2006. p. 277–95.

Kawaguchi Y, Shindou T. Noradrenergic excitation and inhibition of GABAergic cell types in rat frontal cortex. J Neurosci 1998; 18: 6963–76.

Kim T-W, Wu K, Xu J-L, Black IB. Detection of dystrophin in the postsynaptic density of rat brain and deficiency in a mouse model of

Duchenne muscular dystrophy. Proc Natl Acad Sci USA 1992; 89: 11642–4.

Kins S, Betz H, Kirsch J. Collybistin, a newly identified brain-specific GEF, induces submembrane clustering of gephyrin. Nat Neurosci 2000; 3: 22–9.

Knuesel I, Mastrocola M, Zuellig RA, Bornhauser B, Schaub MC, Fritschy JM. Altered synaptic clustering of $GABA_A$ receptors in mice lacking dystrophin (*mdx* mice). Eur J Neurosci 1999; 11: 4457–62.

Komoto J, Usui S, Otsuki S, Terao A. Infantile autism and Duchenne muscular dystrophy. J Autism Dev Disord 1984; 14: 191–5.

LeDoux JE. Emotion circuits in the brain. Annu Rev Neurosci 2000; 23: 155–84.

LeDoux JE, Iwata J, Cicchetti P, Reis DJ. Different projections of the central amygdala nucleus mediate autonomic and behavioral correlates of conditioned fear. J Neurosci 1988; 8: 2517–29.

Levi S, Grady RM, Henry MD, Campbell KP, Sanes JR, Craig AM. Dystroglycan is selectively associated with inhibitory GABAergic synapses but is dispensable for their differentiation. J Neurosci 2002; 22: 4274–85.

Lidov HGW. Dystrophin in the nervous system. Brain Path 1996; 6: 63–77.

Lidov HG, Byers TJ, Kunkel LM. The distribution of dystrophin in the murine central nervous system: an immunocytochemical study. Neuroscience 1993; 54: 167–87.

Lidov HG, Byers TJ, Watkins SC, Kunkel LM. Localization of dystrophin to postsynaptic regions of central nervous system cortical neurons. Nature 1990; 348: 725–8.

Maren S, Fanselow MS. Synaptic plasticity in the basolateral amygdala induced by hippocampal formation stimulation in vivo. J Neurosci 1995; 15: 7548–64.

McDonald AJ, Mascagni F. Parvalbumin-containing interneurons in the basolateral amygdala express high levels of the alpha1 subunit of the GABAA receptors. J Comp Neurol 2004; 473: 137–46.

Miller MM, McEwen BS. Establishing an agenda for translational research on PTSD. Ann N Y Acad Sci 2006; 1071: 294–312.

Muller JF, Mascagni F, McDonald AJ. Postsynaptic targets of somatostatin-containing interneurons in the rat basolateral amygdala. J Comp Neurol 2007; 500: 513–29.

Muntoni F, Mateddu A, Serra G. Passive avoidance behavior deficit in the *mdx* mouse. Neuromuscul Disord 1991; 1: 121–3.

Nakao K, Matsuyama K, Matsuki N, Ikegaya Y. Amygdala stimulation modulates hippocampal synaptic plasticity. Proc Natl Acad Sci USA 2004; 101: 14270–5.

Neri M, Torelli S, Brown S, Ugo I, Sabatelli P, Merlini L, et al. Dystrophin levels as low as 30% are sufficient to avoid muscular dystrophy in the human. Neuromuscul Disord 2007; 17: 913–18.

Papadopoulos T, Korte M, Eulenburg V, Kubota H, Retiounskia M, Harvey RJ, et al. Impaired GABAergic transmission and altered hippocampal synaptic plasticity in collybistin-deficient mice. EMBO J 2007; 26: 3888–99.

Pastoret C, Sebille A. *mdx* mice show progressive weakness and muscle degeneration with age. J Neurol Sci 1995; 129: 97–105.

Pentkowski NS, Blanchard DC, Lever C, Litvin Y, Blanchard RJ. Effects of lesions to the dorsal and ventral hippocampus on defensive behaviors in rats. Eur J Neurosci 2006; 23: 2185–96.

Persohn E, Malherbe P, Richards JG. Comparative molecular neuroanatomy of cloned GABAA receptor subunits in the rat CNS. J Comp Neurol 1992; 326: 193–216.

Rainnie DG, Mania I, Mascagni F, McDonald AJ. Physiological and morphological characterization of parvalbumin-containing interneurons of the rat basolateral amygdala. J Comp Neurol 2006; 498: 142–61.

Roccella M, Pace R, De Gregorio MT. Psychopathological assessment in children affected by Duchenne de Boulogne muscular dystrophy. Minerva Pediatr 2003; 55: 267–76.

Rodriguez Manzanares PA, Isoardi NA, Carrer HF, Molina VA. Previous stress facilitates fear memory, attenuates GABAergic inhibition, and increases synaptic plasticity in the rat basolateral amygdala. J Neurosci 2005; 25: 8725–34.

Ruiz Martinez RC, de Oliveira AR, Brandao ML. Conditioned and unconditioned fear organized in the periaqueductal gray are differentially sensitive to injections of muscimol into amygdaloid nuclei. Neurobiol Learn Mem 2006; 85: 58–65.

Sah P, Faber ESL, Lopez de Armentia M, Power J. The amygdaloid complex: anatomy and physiology. Physiol Rev 2003; 83: 803–34.

Sesay AK, Errington ML, Levita L, Bliss TVP. Spatial learning and hippocampal long-term potentiation are not impaired in *mdx* mice. Neurosci Lett 1996; 211: 207–10.

Sicinski P, Geng Y, Ryder-Cook AS, Barnard EA, Darlison MG, Barbard PJ. The molecular basis of muscular dystrophy in the *mdx* mouse: a point mutation. Science 1989; 244: 1578–80.

Sugita S, Saito F, Tong J, Satz J, Campbell K, Sudhof TC. A stoichiometric complex of neurexins and dystroglycan in brain. J Cell Biol 2001; 154: 435–45.

Suzuki A, Yoshida M, Yamamoto H, Ozawa E. Glycoprotein-binding site of dystrophin is confined to the cysteine-rich domain and the first half of the carboxy-terminal domain. FEBS Lett 1992; 308: 154–60.

Tanabe Y, Esaki K, Nomura T. Skeletal muscle pathology in X chromosome-linked muscular dystrophy (mdx) mouse. Acta Neuropathol (Berl) 1986; 68: 91–5.

Tanaka M, Kohno Y, Nakagawa R, Ide Y, Takeda S, Nagasaki N, Noda Y. Regional characteristics of stress-induced increase in brain noradrenaline release in rats. Pharmacol Biochem Behav 1983; 19: 543–7.

Vaillend C, Billard JM, Laroche S. Impaired long-term spatial and recognition memory and enhanced CA1 hippocampal LTP in the dystrophin-deficient Dmd(*mdx*) mouse. Neurobiol Dis 2004; 17: 10–20.

Vaillend C, Rendon A, Misslin R, Ungerer A. Influence of dystrophin-gene mutation on *mdx* mouse behavior. I. Retention deficits at long delays in spontaneous alteration and bar-pressing tasks. Behav Genet 1995; 25: 569–79.

Wicksell RK, Kihlgren M, Melin L, Eeg-Olofsson O. Specific cognitive deficits are common in children with Duchenne muscular dystrophy. Dev Med Child Neurol 2004; 46: 154–9.

Yamada K, Santo-Yamada Y, Wada E, Wada K. Role of bombesin (BN)-like peptides/receptors in emotional behavior by comparison of three strains of BN-like peptide receptor knockout mice. Mol Psychiatry 2002; 7: 113–17.

Zushida K, Sakurai M, Wada K, Sekiguchi M. Facilitation of extinction learning for contextual fear memory by PEPA – a potentiator of AMPA receptors. J Neurosci 2007; 27: 158–66.